Proc. Natl. Acad. Sci. USA
Vol. 86, pp. 8212–8216, November 1989
Biochemistry

Crystal structure of the Glu-239 → Gln mutant of aspartate carbamoyltransferase at 3.1-Å resolution: An intermediate quaternary structure

(x-ray crystallography/allosteric enzyme/site-directed mutagenesis)

J. ERIC GOUAUX, RAYMOND C. STEVENS, HENGMING KE, AND WILLIAM N. LIPSCOMB

Gibbs Chemical Laboratory, Harvard University, Cambridge, MA 02138

Contributed by William N. Lipscomb, July 20, 1989

ABSTRACT **The structure of the unligated Glu 239 → Gln mutant of *Escherichia coli* aspartate carbamoyltransferase (EC 2.1.3.2) has been determined to 3.1-Å resolution and refined to a crystallographic residual of 0.22 in the space group *P*321. The unit-cell dimensions of the unligated enzyme are *a* = 122.3 Å, *c* = 147.1 Å. The *c* axis cell length is intermediate between the *c* axis lengths of the T (tense) (*c* = 142.2 Å) and R (relaxed) (*c* = 156.2 Å) state structures. Furthermore, the quaternary structure of the mutant enzyme is intermediate between the quaternary structures of the T form and the R form. The differences between the quaternary structures of the Glu-239 → Gln and T-form enzymes can be described as follows: the separation between the catalytic trimers increases by ≈1.5 Å along the threefold axis, and they each rotate in opposite directions ≈0.5° around the threefold axis, whereas the regulatory dimers rotate ≈2° around the twofold axes.**

Poised at the beginning of the pyrimidine biosynthetic pathway, aspartate carbamoyltransferase (from *Escherichia coli*, EC 2.1.3.2.; for review, see ref. 1) commits aspartate to the formation of CTP, UTP, and TTP by catalyzing the reaction between aspartate and carbamoyl phosphate to yield *N*-carbamoyl-L-aspartate and phosphate (2, 3). The holoenyzme is allosterically inhibited by CTP and is activated by ATP (4, 5). Recently, it has been shown that UTP, in combination with CTP, can inhibit the enzyme more than CTP alone (6). High-resolution structures have been determined and thoroughly refined for the CTP-ligated T (tense) state (T^{ctp}) (see abbreviations footnote) (7) and the *N*-phosphonoacetyl-L-aspartate (PALA)-ligated R (relaxed) state (R_{pala}) (8, 9). The quaternary rearrangement accompanying the T → R transition is illustrated in Fig. 1.

The region of the protein that undergoes the most profound conformational rearrangement as a result of the T → R transition is a flexible loop of the catalytic chain composed of residues 230–250 (the 240s loop) (7, 9). Residues from the 240s loop are of cardinal importance to the binding of aspartate (13), the stabilization of the carbamoyl phosphate and aspartate domain interface in the R state (14), and the interaction with residues from the other catalytic trimer participating in the *C*1–*C*4 interface (15, 16). In the T state, the carboxylate of residue Glu-239 in the *C*1 catalytic chain interacts with the side-chain groups of residues Lys-164 and Tyr-165 from the *C*4 catalytic chain, as illustrated in Fig. 2. In addition, the carboxylate of residue Glu-239 forms an intrachain hydrogen bond to the main-chain NH group of Asp-236 in the T^{ctp} and R_{pala} structures. In the R state, the carboxylate of Glu-239 also interacts with the side-chain groups of Lys-164 and Tyr-165 from the same catalytic chain. To test the hypotheses concerning the roles of Glu-239, Ladjimi and Kantrowitz (16) changed the glutamate to a glutamine.

Functionally, the Glu-239 → Gln* holoenzyme is devoid of both homotropic and heterotropic cooperativity; the Hill coefficient is 1.0, and the enzyme is neither inhibited by CTP nor activated by ATP (16). The maximum velocities of the mutant and native holoenzymes are almost identical, whereas the mutant holoenzyme exhibits an increased affinity for aspartate (16). These functional observations led Ladjimi and Kantrowitz (16) to speculate that ". . . the single Glu to (→) Gln change is sufficient to completely destabilize the T state and 'freeze' the enzyme in the R state."

MATERIALS AND METHODS

The Glu-239 → Gln mutant was prepared and purified as described (16). Crystallization of the unligated enzyme was effected by first dialyzing the enzyme from a 1:1 (vol/vol) mixture of glycerol and storage buffer (40 mM K_2HPO_4/2.0 mM 2-mercaptoethanol/0.2 mM EDTA, pH 7.0) into storage buffer. Subsequently, the enzyme concentration was adjusted to 15 mg/ml (the extinction coefficient is 0.59 cm^2/mg at 280 nm), and the solution was filtered through a 0.22-μm filter (Millipore Durapore). The enzyme solution was then placed in microdialysis chambers covered with dialysis membrane, and the dialysis chambers were placed in the crystallization buffer (45 mM maleic acid/45 mM Tris base/1 mM *N*-ethylmorpholine/0.3 mM sodium azide/0.2 mM EDTA, pH 5.8 with NaOH). Typically, thick hexagonal plates of dimensions 0.3 × 0.7 × 0.7 mm grew in 1–2 weeks at 20°C. The crystals belonged to the space group *P*321 with unit cell dimensions of *a* = 122.3 Å and *c* = 147.1 Å. Crystals of the Glu-239 → Gln CTP-ligated enzyme were grown in a similar fashion to the unligated crystals with the addition of 1 mM CTP to the crystallization buffer. The space group of the CTP-ligated Glu-239 → Gln crystals is also *P*321, and the unit-cell dimensions are *a* = 122 Å and *c* = 142 Å.

The publication costs of this article were defrayed in part by page charge payment. This article must therefore be hereby marked "*advertisement*" in accordance with 18 U.S.C. §1734 solely to indicate this fact.

Abbreviations: T, tense form of the enzyme (which has unit cell dimensions of *a* = 122 Å, *c* = 142 Å in space group *P*321); R, relaxed form of the enzyme (which has unit cell dimensions of *a* = 122 Å, *c* = 156 Å also in space group *P*321). Functionally, the T form shows low activity and low aspartate affinity, whereas the R form has high activity and a high affinity for aspartate. [See Monod *et al.* (27) for discussion of a theory of allosteric transitions in proteins and for an explanation of the nomenclature.] To signify that a structure contains a ligand bound at the active site a lowercase abbreviation of the ligand name is added as subscript to either T or R; if the ligand is bound to the regulatory site, the ligand abbreviation is added as superscript. PAM, phosphonoacetamide; PALA, *N*-phosphonoacetyl-L-aspartate.

*The notation used to name a mutant enzyme consists of the wild-type amino acid followed by its numerical location in the sequence at left of arrow, and at right of arrow is the new amino acid; for example, Glu-239 → Gln indicates the glutamic acid at position 239 was changed to a glutamine. The mutant enzyme might also be called the Gln-239 enzyme.

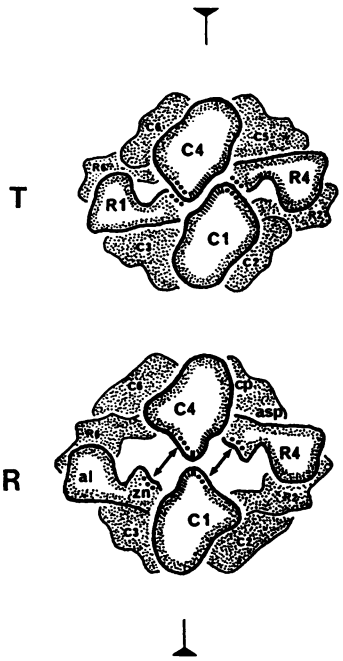

FIG. 1. Shown above is a schematic drawing of the quaternary structures for the canonical T and R states of aspartate carbamoyltransferase. The crystallographic threefold axis is vertical, in the plane of the page. One of the molecular twofold axes lies in the center of the *C*1–*C*4 interface and projects perpendicularly from the plane of the page. Comprising the dodecameric enzyme are two catalytic trimers (*C*1,*C*2,*C*3; *C*4,*C*5,*C*6) and three regulatory dimers (*R*1,*R*6; *R*2,*R*4; *R*5,*R*3) arranged with approximate D_3 symmetry in the *P*321 crystal form discussed in this paper (10). The regulatory dimer composed of chains *R*5 and *R*3 is behind the catalytic trimers and out of view. As a result of the T-to-R transition, the separation of the trimers increases by 12 Å along the threefold axis, while they rotate 5° in opposite directions around the same axis (total rotation 10°); the regulatory dimers rotate by 15° about the three twofold axes (11, 12). The areas defining the *C*1–*C*4 interface are indicated by hatch marks, and the *C*1–*R*4 and *C*4–*R*1 interface regions are depicted by asterisks. Note that the *C*1–*R*4 and *C*4–*R*1 interfaces are abolished in the R state.

X-ray diffraction data on the unligated crystals were collected at the Biotechnology Resource (University of Virginia, Charlottesville), on the multiwire x-ray diffractometer (17) and were processed as described (18), giving an R_{merge} ($R_{merge} = \sum_{hkl}\sum_i|I - \bar{I}|/\sum_i I$) of 0.08 for 34,686 observations of 15,160 unique reflections. The reduced data set is 63% complete in the resolution range 3.1–10.0 Å.

The Glu-239→Gln structure was solved using an approach similar to the "molecular tectonics" method that was applied to the solution of the quaternary structure of the R state (11). Contained in the asymmetric unit of the Glu-239 → Gln crystal in the space group *P*321 are two catalytic and two regulatory chains: one catalytic chain resides on the upper catalytic trimer and one on the lower catalytic trimer, and the two regulatory chains make up the regulatory dimer. The crystallographic threefold operation then generates the holoenzyme (c_6r_6, where *c* represents catalytic and *r* represents regulatory chains). We created a molecular replacement model by partitioning the contents of the asymmetric unit of the T state into three regions: one region consisted of the allosteric domain (residues 8–100 of both regulatory chains) and the other two regions were each composed of one catalytic chain and its associated zinc domain (residues 101–153 of the regulatory chain). Next, the rotations and translations necessary to generate the R-state quaternary structure from the T state were calculated. These rotations and translations were then scaled by the ratio of the difference in the *c* axis length between the Glu-239 → Gln and T-state crystal forms (5 Å) and the difference between the R- and T-state crystal forms (14 Å). This crude calculation gave a scale factor of 0.36 that was then applied to the rotations and translations for the T → R transformation, and the resulting transformations were applied to the T-state regions to yield the beginning molecular replacement model. The initial crystallographic residual ($R_{factor} = \sum_{hkl}||F_o| - |F_c||/|F_o|$) calculated using data between 10 and 4 Å ($I/\sigma(I) \geq 8.0$), was 0.41.

We proceeded to refine the structure using the computer program X-PLOR (19, 20). Initially, we employed rigid-body refinement of the three regions mentioned above to minimize the errors in the final structure (21). Subsequently, we incorporated more observed structure factors, while allowing the model additional degrees of freedom. After further refinement using the simulated annealing method as incorporated into X-PLOR and allowing all atoms to refine subject to energy restraints, the R_{factor} converged to 0.22 for all 15,160 reflections between 3.1 and 10.0 Å. Manual correction of errors in the protein structure based on $(2F_o-F_c)$, on (F_o-F_c), and on omit electron density maps, in addition to the visual inspection of the model, was accomplished with the graphics program FRODO (22), running on an Evans and Sutherland PS300 graphics system interfaced to a VAX 11/780 computer. The resulting structure has good stereochemistry (rms_{bond} = 0.019 Å and rms_{angle} = 3.9°). The restraints used in the refinement consisted of the standard potentials in version 1.5 of X-PLOR (20). Throughout the refinement, the charges on the side-chain groups of the arginine, aspartate, glutamate, lysine, and histidine residues were turned off.

RESULTS

Crystallization of unligated Glu-239 → Gln mutant holoenzyme at pH 5.8 yielded crystals with a hexagonal plate morphology in the space group *P*321 with unit-cell dimensions a = 122.3 Å and c = 147.1 Å. The c cell length is ≈5 Å longer than the c length of T^{ctp} crystals, 2 Å shorter than the c length of phosphate- and aspartate-ligated crystals (23), and ≈9 Å shorter than the c cell length of R_{pala} crystals (24, 25). When crystals of the Gln-239 mutant enzyme were grown in the presence of CTP, we obtained *P*321 crystals with unit-cell dimensions a = 122 Å and c = 142 Å, based on screened precession photographs.

The molecular "tectonics" solution of the Glu-239 → Gln structure has yielded a model with good stereochemistry at moderate resolution. Like the other structures of aspartate carbamoyltransferase, the electron density is strongest in the carbamoyl phosphate domains of the catalytic chains and the zinc domains of the regulatory chains. Also like the other structures, the electron density in the region of the 240s loop is weak. Consequently, for the mutant structure the uncertainty in the positions of residues in and adjacent to the 240s loop is on the order of 1–2 Å. This estimate is based on Luzzati plots (26), on consideration of the refined temperature factors, and on multiple refinements of other aspartate carbamoyltransferase structures, at similar resolution limits (43). The error in the positions of well-resolved groups, such as the domains of the enzyme, will be much smaller than the error in the positions of individual atoms. The secondary and tertiary structure of the refined Glu-239 → Gln model is similar to that of the previously solved T- and R-state structures. However, the quaternary structure of the mutant enzyme is significantly different from both the T and R quaternary structures, although the intermediate conformation is more similar to the T than to the R conformation. The difference between the T and the Glu-239 → Gln structures can be described by an increase in the separation of the catalytic trimers by average values of ≈1.5 Å and rotations about the molecular twofold axes of ≈2°. There is a small

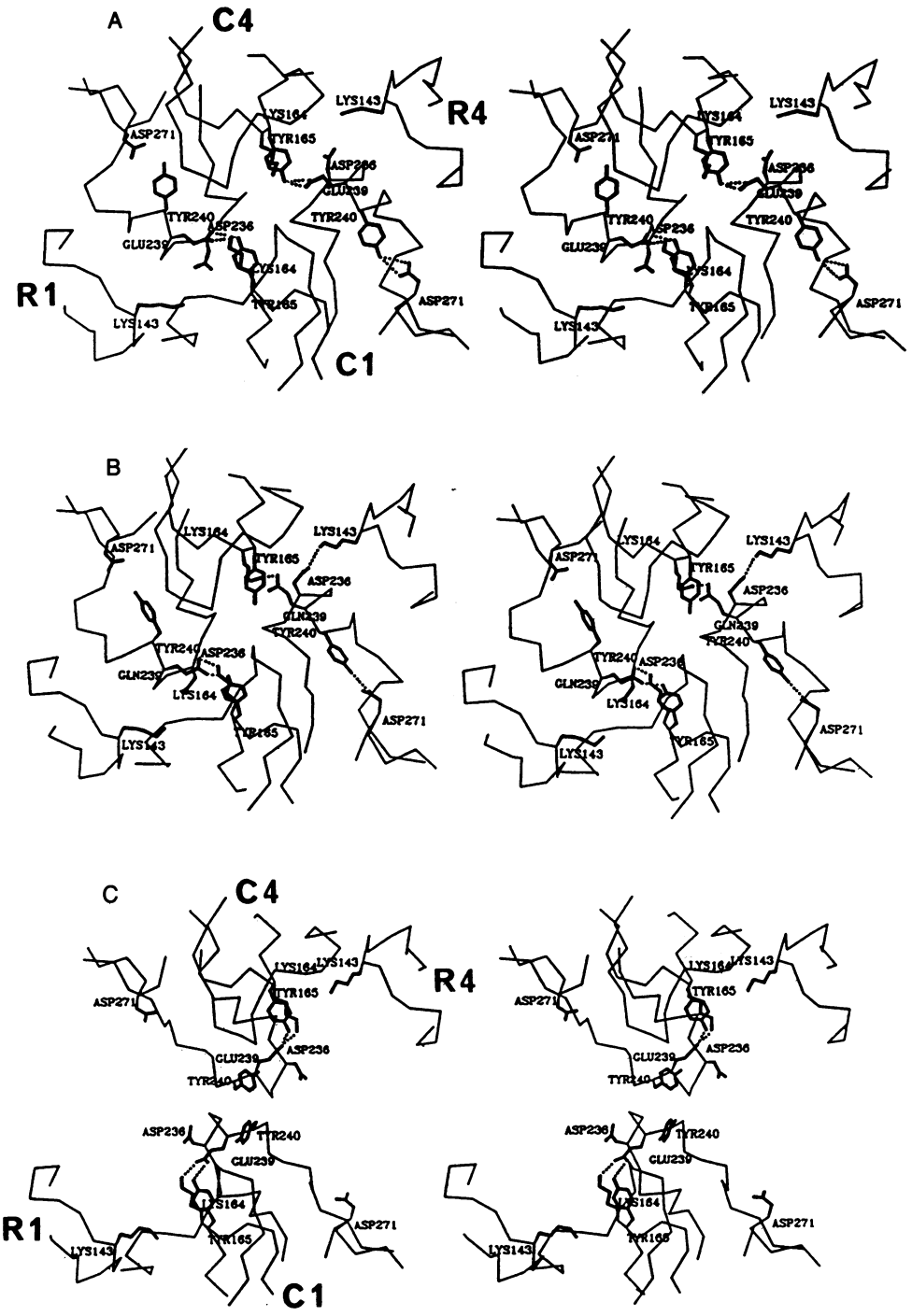

FIG. 2. A stereo drawing of the *C*1–*C*4, *C*1–*R*4, and *C*4–*R*1 interfaces in the T^{ctp} (7) (*A*), the Glu-239 → Gln (*B*), and the R_{pala} (9) (*C*) structures. Only fragments of the α-carbon backbone are drawn along with the selected side chains. Possible hydrogen bonds are indicated by dotted lines. Interactions between the side chain of Glu-239 and the main-chain NH groups are not shown. The threefold axis is vertical, and one of the twofold axes projects perpendicularly out of the plane of the page. This view is similar to the view in Fig. 1. Therefore, *C*1 is the lower chain, *C*4 is the upper chain, *R*1 is the segment in the lower left corner, and *R*4 is the fragment in the upper right corner.

rotation of the catalytic trimers around the threefold axis, each rotating ≈0.5°, in opposite directions, toward their R-state positions. The relative displacement of the upper catalytic chain trimer is shown in Fig. 3. This relatively small reorientation of the catalytic trimers and regulatory dimers, in contrast to the rearrangement that occurs upon the transition to the R state, permits interactions to occur across the *C*1–*C*4 and *C*1–*R*4 interfaces, as documented in Table 1.

DISCUSSION

As hypothesized in both the Monod, Wyman, and Changeux (MWC) (27) and the Koshland, Némethy, and Filmer (KNF) (28) models, interfaces between polypeptide chains in allosteric proteins are important for the manifestation of cooperativity. For example, the catalytic trimers of aspartate carbamoyltransferase will not aggregate to form the c_6 species, presumably because the interactions across the *C*1–*C*4 (Fig. 1) interface are not strong enough to hold the trimers together (29). Addition of three regulatory dimers to one catalytic trimer produces the molecule c_3r_6, in which interactions across *C*1–*R*1 and *C*1–*R*4 interfaces are possible, but which nonetheless shows hyperbolic kinetics and no activation by ATP or inhibition by CTP (30, 31). However, the species c_6r_4, missing one regulatory dimer, possesses homotropic and heterotropic cooperativity (32). In a recent series of mutagenesis experiments done by Schachman and coworkers (33), the change of Asn-111 → Ala in the regulatory chain (near the *C*1–*R*4 interface in the T state) leads to a mutant enzyme with no cooperativity and an R state-like sedimentation coefficient in the presence of 40 mM phosphate, a substrate for the reverse reaction. This information,

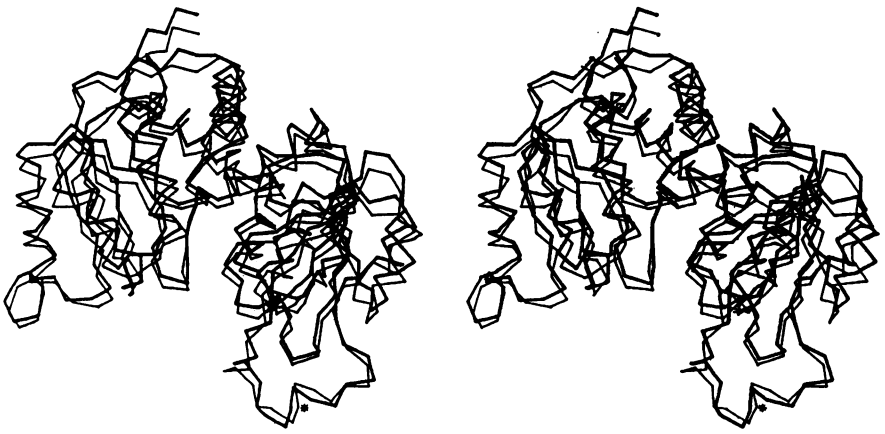

FIG. 3. The relative position of the *C*4 catalytic chain of the Gln-239 enzyme (thick lines) and the *C*4 chain of the T^{c+p} enzyme after the superposition of the *C*1 chains from each structure. The α carbon of residue 239 is to the left of the asterisk.

coupled with the crystallographic studies, implicates the *C*1–*C*4, *C*1–*R*4, *C*4–*R*1, and *C*1–*R*1–*R*6–*C*6 interactions as important for endowing the holoenzyme with homotropic and heterotropic cooperativity. Because the 240s loop defines crucial portions of the *C*1–*C*4, *C*1–*R*4, and *C*4–*R*1 interfaces in the T state and the *C*1–*C*4 interface in the R state, our knowledge of cooperativity in aspartate carbamoyltransferase must include a structural and functional understanding of the 240s loop.

We have determined that the conformation of the enzyme, under the conditions of the crystallization, is intermediate between the T and the R states. There could be at least two reasons for the apparent contradiction between the kinetic and the crystallographic results. In the kinetic studies, the enzyme was saturated with carbamoyl phosphate. Ligation of the enzyme with phosphonoacetamide, a competitive inhibitor of carbamoyl phosphate, produces local conformational changes in the enzyme, the most important probably being the shift in the 50s loop and the formation of a salt link between Glu-50 and Arg-167 (43). Mutagenesis experiments have shown that the interdomain salt link between Glu-50 and Arg-167 is important for stabilizing the R state (15). Also, it is known that carbamoyl phosphate increases the stability of the R state relative to the T state by 2.1 kcal/mol (34). Consequently, for the Gln-239 mutant enzyme, carbamoyl phosphate binding might induce the transition from the unligated quaternary structure to an R-state-like quaternary structure. Of course carbamoyl phosphate may not promote any quaternary conformational changes in the Gln-239 enzyme but rather it might "prepare" the active sites such that the transition to the R state occurs upon binding of the first aspartate molecule.

Table 1. Interactions between residue 239 in the T^{c+p}, Gln-239, and R_{pala} structures.

	Residue		
	Residue I	Residue II	Distance, Å
T state	*C*1 Glu-239 OE1	*C*1 Asp-236 N	2.7
	*C*1 Glu-239 OE2	*C*4 Lys-164 NZ	5.1
	*C*1 Glu-239 OE1	*C*4 Tyr-165 OH	2.8
	*C*1 Glu-239 OE2	*C*4 Tyr-165 OH	3.2
	*C*4 Glu-239 OE2	*C*4 Asp-236 N	2.7
	*C*4 Glu-239 OE2	*C*1 Lys-164 NZ	2.9
	*C*4 Glu-239 OE2	*C*1 Tyr-165 OH	3.3
	*C*4 Glu-239 OE1	*C*1 Tyr-165 OH	3.1
Gln-239	*C*1 Gln-239 OE1	*C*4 Lys-164 NZ	3.0
	*C*1 Gln-239 NE2	*C*4 Tyr-165 OH	4.0
	*C*4 Gln-239 OE1	*C*1 Lys-164 NZ	3.0
	*C*4 Gln-239 OE1	*C*1 Tyr-165 OH	3.0
R state	*C*1 Glu-239 OE2	*C*1 Asp-236 N	3.1
	*C*1 Glu-239 OE2	*C*4 Lys-164 NZ	2.8
	*C*1 Glu-239 OE2	*C*4 Tyr-165 OH	2.9
	*C*1 Glu-239 OE1	*C*4 Tyr-165 OH	3.2
	*C*4 Glu-239 OE2	*C*4 Asp-236 N	2.8
	*C*4 Glu-239 OE1	*C*1 Lys-164 NZ	2.8
	*C*4 Glu-239 OE2	*C*1 Tyr-165 OH	2.6
	*C*4 Glu-239 OE1	*C*1 Tyr-165 OH	3.0

OE, carboxylate oxygen; NE, primary amide nitrogen; NZ, amine nitrogen.

If *C*1 Glu-239 stabilizes the T state by interacting with *C*4 Lys-164 and *C*4 Tyr-165 as shown in Fig. 2, then the mutation of Lys-164 or Tyr-165 to residues incapable of hydrogen bonding might produce an enzyme that is similar to the Glu-239 → Gln mutant. Although chemical modification experiments (35) and mutation of Tyr-165 to serine (36) have already been done, the drastic nature of these alterations unnecessarily complicates their interpretation, particularly since Tyr-165 was recently changed to a phenylalanine (37). Surprisingly, the Tyr-165 → Phe enzyme has near normal homotropic and heterotropic cooperativity and maximum velocity, but it has a substantially decreased affinity for aspartate; the substrate concentration at half the maximum observed specific activity $[S]_{0.5}$ is 90 mM for the mutant compared with 5.5 mM for the native holoenzyme at pH 7.0 (37). The aspartate K_m for the Tyr-165 → Phe catalytic trimer is 16.5 mM compared to 8.0 mM for the native trimer. Ladjimi and Kantrowitz (16) found the aspartate K_m for the Glu-239 → Gln mutant trimer to be 21.9 mM in contrast to 5.9 mM for the native trimer. Assuming that the intrachain interactions between Glu-239, Lys-164, and Tyr-165 in the R-state structure are similar to their interactions in the isolated catalytic trimer after aspartate binding, we could speculate that the perturbation of the triad by mutation might alter the position of the 240s loop, which would then effect the binding of aspartate. Therefore, in the context of this model, we can understand why the Phe-165 and Gln-239 mutant trimers have a reduced affinity for aspartate.

Furthermore, if the substrate concentration at half the maximum observed specific activity measures the Gln-239 holoenzyme's affinity for aspartate, then the holoenzyme has a higher affinity for aspartate than does the catalytic trimer. Indeed, we might also predict that the mutation of Tyr-165 to phenylalanine should produce a similar effect: a holoenzyme with diminished cooperativity and a higher affinity for aspartate. However, this is not the case: the Tyr-165 → Phe holoenzyme has a substantially decreased affinity for aspartate. These results imply that the interactions between Glu-239, Lys-164, and Tyr-165 might not be as simple and symmetrical as originally envisioned. Although the carbox-

ylate of *C*1 Glu-239 in the T^{ctp} structure is too far from the amino group of *C*4 Lys-164 to form a salt link, in a T-state structure determined at pH 7.0 these side chains are close enough to form a salt link (43). We know from the T^{ctp} and R_{pala} structures that Glu-239 forms an intrachain hydrogen bond to the main-chain NH group of Asp-236. This interaction is probably important for the stabilization of the secondary structure between Asp-236 and Asn-242. Therefore, the role of Glu-239 in the stabilization of the T and R states might not be limited to its intertrimer and intratrimer interactions with Lys-164 and Tyr-165, but it might also include the intrachain hydrogen bond to Asp-236. In the Gln-239 structure, the side-chain of Gln-239 is too far from the NH of Asp-236 to form a hydrogen bond. The absence of this interaction might be one of the factors that allows the 240s loop to extend slightly while maintaining contacts with residues 164 and 165 from the other catalytic trimer as the trimers separate by ≈1.5 Å. Although the intermediate Gln-239 structure emphasizes the importance of Glu-239 in the stabilization of the T state, its precise role and the roles of Lys-164 and Tyr-165 are not yet clear. As has been recently shown by Karplus and coworkers in the computational analysis of a mutant hemoglobin (38), the decomposition of the multiple effects of a mutation can be a complex process.

The extension of the 240s loop in the Gln-239 structure means that even though the catalytic trimers have separated ≈1.5 Å, residues bridging the *C*1–*C*4, *C*1–*R*4, and *C*4–*R*1 interfaces can still interact, as illustrated in Fig. 2. Specifically, we observe a salt link between *C*1 Asp-236 and R4 Lys-143 and a hydrogen bond between *C*4 Ser-238 and *R*1 Lys-143. We speculate that these interactions provide a mechanism for the growth of CTP-ligated Glu-239 → Gln crystals that have a *c* unit-cell dimension that is identical to the *c* axis length of native CTP-ligated crystals. Molecules that bind to the active site, such as aspartate and carbamoyl phosphate, probably overwhelm the weaker effects of ATP and CTP and consequently preclude the observation of heterotropic cooperativity in kinetic experiments.

The pAR5 aspartate carbamolytransferase mutant has the last eight residues of the regulatory chain, near the *C*1–*R*4 and *C*4–*R*1 interfaces in the T state, replaced by six different residues (39). This enzyme shares some similarities with the Glu-239 → Gln mutant (40). The unligated enzyme quaternary structure is intermediate between the T and R states as determined by x-ray scattering in solution (41). This very low-resolution structural study, combined with molecular mechanics calculations, further implicates the *C*1–*R*4, *C*4–*R*1 and possibly the zinc–allosteric domain interfaces in the manifestation of the homotropic and heterotropic cooperativity.

Although previous studies have indicated that the quaternary structure of the enzyme in the crystal is similar to its structure in solution (42), the Glu-239 → Gln enzyme might be more susceptible to the intermolecular contacts in the crystal. Consequently, the structure of the mutant enzyme in the crystal might prove different from its structure in solution.

Prof. E. R. Kantrowitz and the members of his laboratory are gratefully acknowledged for supplying the mutant enzyme used in this study. We also thank R. H. Kretsinger, S. Sobottka, R. Chandros, and T. Ptak for the use of the Biotechnology Resource at the University of Virginia for collection of the x-ray diffraction data. We thank Axel Brünger for helping to set up X-PLOR on the CRAY YMP at the Pittsburgh Supercomputer Center (PSC). We acknowledge the support of the PSC (Grant CHE880077P) for computer resources, which greatly accelerated the refinements, and the National Institutes of Health (Grant GM06920) for support.

1. Kantrowitz, E. R. & Lipscomb, W. N. (1988) *Science* **241**, 669–674.
2. Jones, M. E., Spector, L. & Lipmann, F. (1955) *J. Am. Chem. Soc.* **77**, 819–820.
3. Reichard, P. & Hanshoff, G. (1956) *Acta Chem. Scand.* **10**, 548–566.
4. Yates, R. A. & Pardee, A. B. (1956) *J. Biol. Chem.* **221**, 757–770.
5. Gerhart, J. C. & Pardee, A. B. (1962) *J. Biol. Chem.* **237**, 891–896.
6. Wild, J. R., Loughrey-Chen, S. J. & Corder, T. S. (1989) *Proc. Natl. Acad. Sci. USA* **86**, 46–50.
7. Kim, K. H., Pan, Z., Honzatko, R. B. & Lipscomb, W. N. (1987) *J. Mol. Biol.* **196**, 853–875.
8. Krause, K. L., Volz, K. W. & Lipscomb, W. N. (1987) *J. Mol. Biol.* **193**, 527–553.
9. Ke, H., Lipscomb, W. N., Cho, Y. & Honzatko, R. B. (1988) *J. Mol. Biol.* **204**, 725–747.
10. Wiley, D. C. & Lipscomb, W. N. (1968) *Nature (London)* **218**, 1119–1121.
11. Ladner, J. E., Kitchell, J. P., Honzatko, R. B., Ke, H. M., Volz, K. W., Kalb (Gliboa), A. J., Ladner, R. C. & Lipscomb, W. N. (1982) *Proc. Natl. Acad. Sci. USA* **79**, 3125–3128.
12. Krause, K. L., Volz, K. W., & Lipscomb, W. N. (1985) *Proc. Natl. Acad. Sci. USA* **82**, 1643–1647.
13. Middleton, S. A., Stebbins, J. W. & Kantrowitz, E. R. (1989) *Biochemistry* **82**, 1617–1626.
14. Middleton, S. A. & Kantrowitz, E. R. (1988) *Biochemistry* **27**, 8653–8660.
15. Ladjimi, M. M., Middleton, S. A., Kelleher, K. S. & Kantrowitz, E. R. (1988) *Biochemistry* **27**, 268–276.
16. Ladjimi, M. M. & Kantrowitz, E. R. (1988) *Biochemistry* **27**, 276–283.
17. Sobottka, S. E., Cornick, G. G., Kretsinger, R. H., Rains, R. G., Stephens, W. A. & Weissman, L. J. (1984) *Nucl. Instrum. Methods* **220**, 575–581.
18. Gouaux, J. E., Lipscomb, W. N., Middleton, S. A. & Kantrowitz, E. R. (1989) *Biochemistry* **28**, 1798–1803.
19. Brünger, A. T., Kuriyan, J. & Karplus, M. (1987) *Science* **235**, 458–460.
20. Brünger, A. T. (1988) *X-PLOR Manual* (Yale Univ., New Haven, Ct), Version 1.5.
21. Derewenda, Z. S. (1989) *Acta Crystallogr.* **A45**, 227–234.
22. Jones, T. A. (1982) in *Computational Crystallography*, ed. Sayre, D. (Oxford Univ. Press, London), pp. 303–317.
23. Gouaux, J. E. & Lipscomb, W. N. (1989) *Proc. Natl. Acad. Sci. USA* **86**, 845–848.
24. Monaco, H. L. (1978) Dissertation (Harvard Univ., Cambridge, MA).
25. Monaco, H. L., Crawford, J. L. & Lipscomb, W. N. (1978) *Proc. Natl. Acad. Sci. USA* **75**, 5276–5280.
26. Luzzati, V. (1952) *Acta Crystallogr.* **5**, 802–810.
27. Monod, J., Wyman, J. & Changeux, J.-P. (1965) *J. Mol. Biol.* **12**, 88–118.
28. Koshland, D. E., Jr., Némethy, G. & Filmer, D. (1966) *Biochemistry* **5**, 365–385.
29. Gerhart, J. C. & Schachman, H. K. (1965) *Biochemistry* **4**, 1054–1062.
30. Mort, J. S. & Chan, W. W.-C. (1975) *J. Biol. Chem.* **249**, 653–660.
31. Chan, W. W.-C. (1975) *J. Biol. Chem.* **250**, 661–667.
32. Evans, D. R., Pastra-Landis, S. C. & Lipscomb, W. N. (1974) *Proc. Natl. Acad. Sci. USA* **71**, 1351–1355.
33. Eisenstein, E., Markby, D. W. & Schachman, H. K. (1989) *Proc. Natl. Acad. Sci. USA* **86**, 3094–3098.
34. Howlett, G. J., Blackburn, M. N., Compton, J. G. & Schachman, H. K. (1977) *Biochemistry* **16**, 5091–5099.
35. Lauritzen, A. M., Landfear, S. M. & Lipscomb, W. N. (1980) *J. Biol. Chem.* **255**, 602-607.
36. Robey, E. A. & Schachman, H. K. (1984) *J. Biol. Chem.* **259**, 11180–11183.
37. Wales, M. E., Hoover, T. A. & Wild, J. R. (1988) *J. Biol. Chem.* **263**, 6109–6114.
38. Gao, J., Kuczera, K., Tidor, B. & Karplus, M. (1989) *Science* **244**, 1069–1072.
39. Cunin, R., Jacobs, A., Charlier, D., Crabeel, M., Hervé, G., Glansdorff, N. & Piérard, A. (1985) *J. Mol. Biol.* **186**, 707–713.
40. Ladjimi, M. M., Ghelis, C., Feller, A., Cunin, R., Glansdorff, N., Piérard, A. & Hervé, G. (1985) *J. Mol. Biol.* **186**, 715–724.
41. Cherfils, J., Vachette, P., Tauc, P. & Janin, J. (1987) *EMBO J.* **6**, 2843–2847.
42. Altman, R. B., Ladner, J. E. & Lipscomb, W. N. (1982) *Biochem. Biophys. Res. Commun.* **108**, 592–595.
43. Gouaux, J. E. & Lipscomb, W. N. (1989) *Biochemistry*, in press.